20th Australasian Fluid Mechanics Conference
Perth, Australia
5-8 December 2016

Sensitivity of Instability Mechanisms to Trailing-Edge Boundary Conditions in High-pressure Turbine Flows

R. D. Sandberg[1] and A. P. S. Wheeler[2]

[1]Department of Mechanical Engineering
University of Melbourne, Victoria 3010, Australia

[2]Department of Engineering
University of Cambridge, Cambridge, U.K.

Abstract

Multi-dimensional linear stability analyses were conducted using forced compressible Navier–Stokes simulations. The base flows were obtained from a previously conducted direct numerical simulation of a high-pressure turbine vane at $Re = 0.57 \times 10^6$ and $M = 0.9$, and from an additional two-dimensional simulation of the same configuration with trailing-edge blowing. The latter case does not exhibit pressure waves originating from the trailing edge impinging on the suction side of the adjacent blade. For the case without trailing-edge blowing, the temporal pulse response reveals the presence of an acoustic feedback loop with amplitude increasing quickly over time. It is also found that the base flow is globally unstable with respect to three-dimensional instabilities, regardless of the perturbation location. In contrast, the case with trailing-edge blowing appears to be stable with regards to two- and three-dimensional disturbances, i.e. it is seen for the first time that the removal of the trailing-edge recirculation region suppresses the acoustic feedback loop and the growth of three-dimensional instabilities.

Introduction

The high-pressure turbine (HPT) of a jet engine typically is subject to the highest temperatures, pressures, and velocities anywhere in the engine. The flow physics are complex as HPTs operate at both transonic Mach numbers and high Reynolds numbers. Measurements are expensive and often unable to provide sufficient insight into the underlying physics. To compensate for the aero-thermal loading uncertainty, designers are forced to incorporate safety margins to ensure adequate turbine performance and reliability. A better understanding and prediction capability of how turbulence affects both the aerodynamic efficiency and the heat transfer from gas to the blades is therefore required. Recently, Wheeler *et al.* [1] performed direct numerical simulations (DNS) of an HPT vane at engine-representative conditions, $Re = 0.57 \times 10^6$ and $M = 0.9$, with blade loads and kinetic loss showing good agreement with laboratory measurements [2]. The simulations revealed that the boundary-layer on the suction side interacts with pressure waves travelling upstream the throat. It was suggested that these waves are triggered by trailing-edge vortex shedding and perturb the suction side boundary layer resulting in a Kelvin–Helmholtz instability that ultimately leads to formation of lambda structures and turbulence, rapidly increasing heat transfer loads.

In the current study, the role of the trailing-edge vortex shedding and near-wake recirculation region on the generation of upstream traveling pressure waves, and their potential for perturbing the suction side boundary layers is investigated. To that end a global linear stability analysis is performed in form of a temporal pulse response using forced Navier–Stokes simulations for base flows obtained from the original 3D DNS. An additional two-dimensional DNS was conducted with trailing-edge blowing in order to provide a baseflow resulting from a case without trailing-edge recirculation. The main focus is on elucidating the effect of the trailing-edge vortex shedding and recirculation on the global instability mechanisms.

Numerical Setup

Boundary Conditions and Grid

The current study considers a linear cascade configuration, thus in the pitchwise direction periodic boundary conditions were used. The solid boundaries on the vane were treated as a no-slip isothermal wall with the wall temperature set to be $T_w = 1.3\,T_{o_{in}}$ to match the experimental data. A zonal characteristic boundary-condition [3] was applied over the final 95 streamwise grid lines to attenuate acoustic reflections from vortical structures passing through the outlet boundary. For the case with trailing-edge blowing, the no-slip wall boundary condition was replaced with

$$u = 0.5\ ;\ v = -0.5 \cdot \tan(1.309) \qquad (1)$$

in the region with $x > 0.975$ and $y < -1.43$. All quantities presented in this paper are non-dimensionalized: Lengths and distances are divided by the axial chord and all other quantities are normalized by reference inlet conditions.

The grid used in the current study is the same as the 'fine mesh' used in the original DNS study presented in Wheeler *et al.* [1], containing a total of 2.5 million points in the blade-to-blade plane. The average near wall grid spacings were $y_1^+ = 0.8, \Delta z^+ = 5, \Delta x^+ = 15$. This grid was used for the forced Navier–Stokes simulations and for the additional two-dimensional DNS with trailing-edge blowing.

Direct Numerical Simulations

An additional 2D DNS was conducted with trailing-edge blowing to provide a base flow for additional stability analysis. The compressible Navier–Stokes equations for conservative variables were solved in curvilinear coordinates using a 4^{th}-order central difference scheme with Carpenter boundary stencils for the spatial discretization in the axial and pitchwise directions. An ultra-low-storage 4^{th}-order Runge–Kutta scheme was used for time-integration and stability of the code was enhanced by a skew-symmetric splitting of the nonlinear terms. In addition, an 11 point wave-number optimized filter was used after each full Runge–Kutta cycle with a weighting of 0.2 to remove possible grid-to-grid-point oscillations. More details about the code and its validation can be found in Sandberg *et al.* [4].

Linear Stability Analysis

A multi-dimensional stability analysis was conducted using forced Navier–Stokes simulations. At the start of each simulation, at $t = 0$, the right-hand-side of the Navier–Stokes equations, containing all spatial derivatives of the base flow as de-

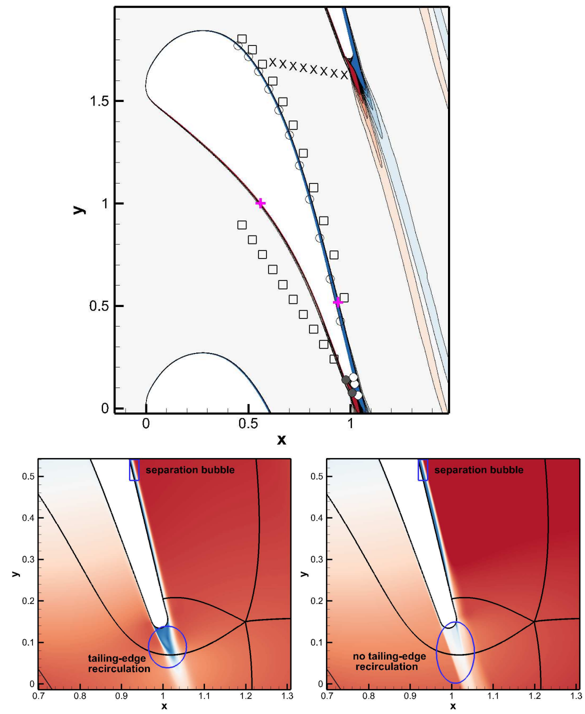

Figure 1: Top: Contours of time-averaged spanwise vorticity component of 3D DNS showing perturbation locations for stability analysis and locations where time-histories were recorded. Bottom: Contours of time-averaged velocity magnitude in trailing-edge region obtained from 3D DNS (left) and 2D DNS with trailing-edge blowing (right).

tailed in Sandberg [5], is computed and stored. The simulation is then progressed, subtracting the stored forcing term for the entire blade-to-blade plane at each Runge–Kutta substep.

The result is that assuming there is no change or perturbation to the flow field, the initial condition can be maintained as a reference state, upon which the behaviour of small perturbations can be investigated. This method has been successfully used for stability investigations of airfoil and wake flows [6, 5]. In the current case, an initial low-amplitude perturbation is added to the simulation and the pulse-response in each case is evaluated. For the stability analyses, the same numerical procedure and the same grids were used as for the DNS. For the three-dimensional stability analysis, a Fourier representation of the spanwise direction was used and all higher Fourier modes were perturbed at the same in-plane location. Note that in the 3D cases, the stored forcing term is only subtracted from the zeroth spanwise Fourier mode.

Results

All simulations presented here were conducted at Reynolds number $Re = 0.57 \times 10^6$ and exit Mach number of 0.9, representative of a modern transonic high-pressure turbine nozzle. These flow conditions and the geometry are those of the previously conducted DNS [1], based on the MUR226 case of the experimental study by Arts *et al.* [2].

Base Flow

The baseflow for the stability investigation was determined using time-series data over at least 4 flow through times. In figure 1 the base flow obtained from the 3D DNS is shown by means of contours of the time-averaged spanwise vorticity component. The forcing locations discussed in this paper, one within the suction side separation bubble at $(x,y) = (0.936582, 0.473511)$, and one in the pressure side boundary layer at $(x,y) = (0.530556, 1.039626)$ are denoted by purple pluses. The open circles denote monitor locations in the suction side boundary layer, open squares denote probes outside of the boundary layers on the suction and pressure sides. X denote monitor points in the vane passage to track trailing-edge noise on the pressure side impinging on the adjacent blade. Other symbols show additional probe locations, however, those are not discussed in the current paper. The base flows for the cases with and without trailing-edge blowing are contrasted in the bottom two figures of figure 1. It can be observed that the case with trailing-edge blowing does not feature a recirculation region in the near wake and it appears as if the suction-side separation bubble (denoted by box) is larger in size than in the 3D DNS (without blowing). In instantaneous snapshots of the flow field (not shown for brevity) it can also be observed that the trailing-edge blowing suppresses pressure waves originating from the trailing edge and impinging on the suction side of the adjacent blade.

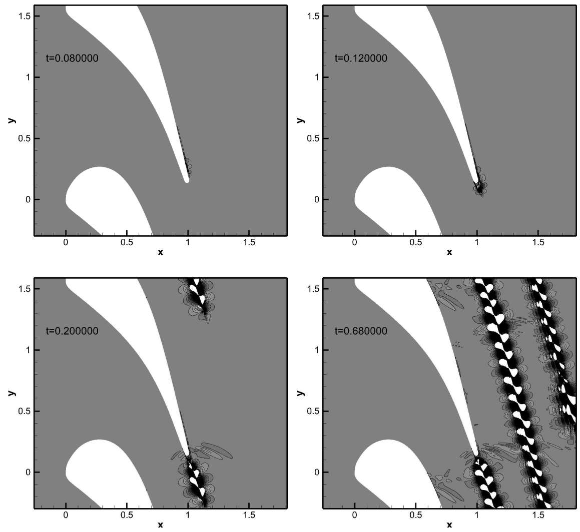

Figure 2: Time history of v-velocity perturbation for 2D forced DNS using base flow from time-averaged 3D DNS, initial pulse in suction side separation bubble; contour levels $[-2 \times 10^{-3}; 2 \times 10^{-3}]$.

Stability Analysis

The multi-dimensional stability analysis via forced direct numerical simulations was performed for two different base flows. The first base flow was obtained from the time- and spanwise averaged DNS solution presented in Wheeler *et al.* [1]. A base flow was also obtained from a two-dimensional simulation using trailing-edge blowing. The main objective for considering trailing-edge blowing was the removal of the strong vortex shedding of the initial wake, which was found to generate upstream traveling pressure waves potentially perturbing the suction side boundary layers in the original DNS. As this vortex shedding and the resulting upstream traveling pressure waves were predominantly two-dimensional phenomena, it was deemed sufficient performing only two-dimensional simulations of the trailing-edge blowing case to obtain the additional base flow. Importantly, it should be noted that care was taken to ensure that the overall blade loading of the additional case with trailing-edge blowing agreed well with the 3D DNS case.

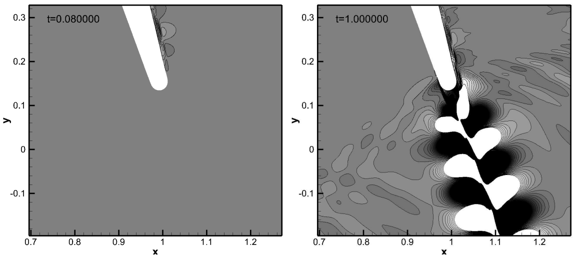

Figure 3: Time history of v-velocity perturbation for 2D forced DNS using base flow from time-averaged 3D DNS, initial pulse in suction side separation bubble, zoom-in on trailing-edge region; contour levels $[-2\times10^{-3}; 2\times10^{-3}]$.

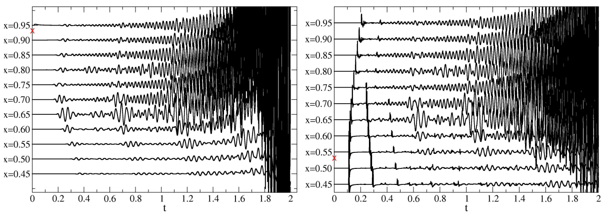

Figure 4: Time history of pressure at various monitor point locations in the suction-side freestream, denoted by open squares in figure 1, from 2D forced DNS with forcing location in the suction side separation bubble (left) and on the pressure side (right) using base flow obtained from time-averaged 3D DNS.

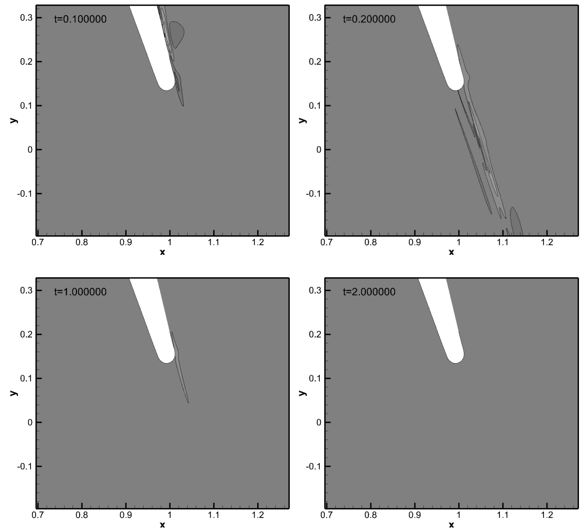

Figure 5: Time history of v-velocity perturbation for 2D forced DNS using base flow from time-averaged 2D DNS with trailing-edge blowing, initial pulse in suction side separation bubble; contour levels $[-2\times10^{-3}; 2\times10^{-3}]$.

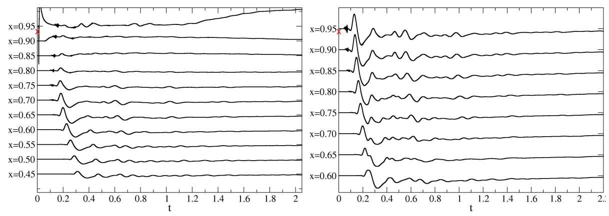

Figure 6: Time history of pressure at various monitor point locations in the suction-side freestream, denoted by open squares in figure 1 (left) and monitor points in the vane passage, denoted by X in figure 1 (right), from 2D forced DNS using base flow obtained from 2D DNS with trailing-edge blowing.

Figure 2 shows snapshots of the temporal response of the 2D mode with respect to an initial pulse, imposed at $t = 0$ on the base flow within the suction side separation bubble with amplitude 10^{-8}. At $t = 0.08$, a wave packet that results from the initial pulse can be seen convecting towards the trailing edge. At the two subsequent time instances, the disturbance continues to convect downstream and temporal growth, in particular in the wake, is evident. At $t = 0.68$ acoustic disturbances, generated by the interaction of the disturbances with the trailing edge, so-called trailing-edge noise, can be seen impinging on the suction side of the adjacent blade. Zooming into the trailing-edge region, see figure 3, reveals that the acoustic perturbation of the suction side boundary layer leads to another wave packet convecting over the trailing edge (see $t = 0.68$). For a more quantitative assessment of the stability behavior, time histories of pressure are show in figure 4 for locations outside of the suction side boundary layer, with the red crosses showing the forcing locations. Two general observations can be made. Firstly, discrete wave packets can be seen to convect up- and downstream. Secondly, overall, all disturbances grow in time. This behavior is reminiscent of what was found for a NACA0012 airfoil at $Re = 50,000$ [6] and indicates the presence of an acoustic feedback loop. Several additional stability simulations were conducted varying the initial pulse location. In figure 4 data is also shown for the case that was perturbed within the pressure side boundary layer. The pressure signals obtained from this case, and for others with perturbations placed in the wake and close to the leading edge, show qualitatively the same behavior, i.e. the presence of an acoustic feedback loop with amplitudes quickly growing to reach saturation levels (and rendering the forced DNS approach meaningless beyond this point).

Snapshots of the temporal response of the 2D mode with respect to an initial pulse with amplitude 10^{-8} imposed at $(x, y) = (0.936582, 0.473511)$ for the base flow from the simulation with trailing-edge blowing is shown in figure 5. At $t = 0.1$ and $t = 0.2$, the initial wave packet can be seen convecting over the trailing edge and into the near wake. However, in contrast to the case without trailing-edge blowing, no temporal growth appears to occur and by $t = 2.0$, nearly three times longer than the time series shown in figure 2, all perturbations have convected out of the domain and no more disturbances can be seen. This is also seen in the time histories of pressure outside of the suction side boundary layer, shown in figure 6. The initial pulse can be seen propagating mainly upstream and some additional wave packets are visible at later times at the upstream positions, albeit at quickly decreasing amplitude. This is characteristic of 'stable acoustic feedback loops' as also observed for airfoils in freestream, e.g. in Jones and Sandberg [7]. Crucially, communication with the suction side boundary layer of the adjacent blade does not seem to occur, as evidenced by the temporal decay in amplitude of all disturbances in the vane passage, as seen in figure 6. This means that the removal of the recirculation region in the near wake prevents the acoustic feedback loop from establishing a globally unstable behavior. It also suggests that the suction side separation bubble is not responsible for the globally unstable behavior observed for the baseline 3D DNS case as it is not removed by the trailing-edge blowing; on the contrary, it is even enlarged. Thus, it can be concluded that the trailing-edge recirculation region is mainly responsible for the observed globally unstable behavior, driven by an acoustic feedback loop.

In order to investigate the stability characteristics of the two

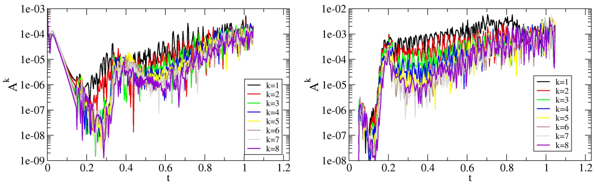

Figure 7: Temporal development of spanwise Fourier modes of density at forcing location (left) and in wake (right) obtained using base flow from time-averaged 3D DNS.

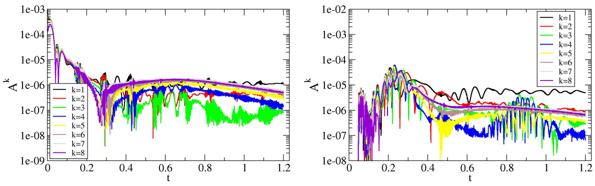

Figure 8: Temporal development of spanwise Fourier modes of density at forcing location (left) and in wake (right) obtained using base flow from 2D DNS with trailing-edge blowing.

base flows discussed above with respect to three-dimensional perturbations, three-dimensional forced DNS were conducted to study the pulse response (initial pulse at $t = 0$ with amplitude 10^{-8} was added to all Fourier modes k). Stability simulations were conducted for several spanwise domain sizes, all producing consistent results, thus only data from calculations with a spanwise extent of 0.4 axial chords are shown, using a total of 8 Fourier modes. Figure 7 shows the pulse response of all spanwise Fourier modes for the case where the base flow obtained from the 3D DNS is perturbed in each spanwise mode within the suction side separation bubble at $(x, y) = (0.936582, 0.473511)$. At the forcing location, all mode amplitudes initially decay until exhibiting strong temporal growth for approximately $t > 0.2$. Based on this and snapshots of the temporal evolution of the individual modes (not shown for brevity), and supported by the findings from the two dimensional stability analysis presented above, it is conjectured that the separation bubble itself is not absolutely unstable but the underlying acoustic feedback loop supports the temporal growth of the three-dimensional modes.

The temporal development of the spanwise Fourier modes in the wake of the vane, several trailing-edge thicknesses downstream of the trailing edge, is also shown in figure 7. Temporal growth of all modes occurs earlier than farther upstream and with a greater growth rate, which supports the above suggestion that the recirculation region of the near wake can be considered to be an amplifier responsible for a globally unstable behavior.

The three dimensional stability investigations were repeated for the base flow obtained from the 2D DNS with trailing-edge blowing with results shown in figure 8. At the forcing location in the suction side separation bubble, the amplitude of all modes decays over time indicating that the base flow is absolutely stable with respect to three dimensional disturbances. In the wake, growth of all modes is observed from roughly $t = 0.1$ until $t = 0.25$ after which the amplitudes decay again. Thus, similar to the two dimensional mode, the effect of trailing edge blowing is the suppression of the global instability of the higher modes as a result of the removal of the near-wake recirculation region. All three-dimensional stability calculations were repeated inserting the initial pulse at other locations and it was found that the results are independent of forcing location.

Conclusions

Time- and spanwise averaged data from DNS of a high-pressure turbine vane at engine-representative conditions were used as base flow for multi-dimensional linear stability analysis. Furthermore, a 2D DNS was conducted of the same HPT vane configuration with trailing-edge blowing to provide an additional base flow without near-wake recirculation region. The multi-dimensional stability analyses were conducted by computing the temporal pulse response of the 2D and 3D spanwise Fourier modes with respect to both base flows.

For the case without trailing-edge blowing, the temporal pulse response of 2D perturbations reveals the presence of an acoustic feedback loop, with rapidly growing amplitudes. The base flow is also found to be globally unstable with respect to 3D instabilities, regardless of the initial perturbation location. When repeating the linear stability simulations with the base flow obtained from the case with trailing-edge blowing, in which the near-wake recirculation region is removed, both 2D and 3D disturbances decay over time, independent of forcing location. This indicates that the trailing-edge recirculation region is largely responsible for the occurrence of the acoustic feedback loop and the rapid temporal growth of three-dimensional disturbances. We have therefore shown that trailing-edge blowing can suppress the acoustic feedback loop.

Acknowledgements

The authors are grateful for the computing resources provided by the Partnership for Advanced Computing in Europe (PRACE), “The Pawsey Supercomputing Centre” with funding from the Australian Government and the Government of Western Australia and the UK Turbulence Consortium under EPSRC grant EP/L000261/1.

References

[1] A. Wheeler, R. Sandberg, N. Sandham, R. Pichler, V. Michelassi and G. Laskowski, Direct Numerical Simulations of a High-Pressure Turbine Vane, *J. Turbomachinery* **138**, 071003 (2016).

[2] T. Arts, R. Lambert and A. W. Rutherford, *Aero-Thermal Investigation of a Highly Loaded Transonic Linear Turbine Guide Vane Cascade*, von Karman Institute Technical Note, Vol. 174, Brussels, Belgium (1990).

[3] R. D. Sandberg and N. D. Sandham, Nonreflecting zonal characteristic boundary condition for direct numerical simulation of aerodynamic sound, *AIAA J.* **44**, 402 (2006).

[4] R. Sandberg, R. Pichler, L. Chen, R. Johnstone and V. Michelassi, Compressible Direct Numerical Simulation of Low-Pressure Turbines: Part I – Methodology, *J. Turbomachinery* **137**, 051011 (2015).

[5] R. D. Sandberg, Numerical investigation of turbulent supersonic axisymmetric wakes, *J. Fluid Mech.* **702**, 488 (2012).

[6] L. E. Jones, R. Sandberg and N. Sandham, Stability and receptivity characteristics of a laminar separation bubble on an aerofoil, *J. Fluid Mech.* **648**, 257 (2010).

[7] L. E. Jones and R. Sandberg, Numerical analysis of tonal airfoil self-noise and acoustic feedback-loops, *J. Sound and Vibration* **330**, 6137 (2011).